

2D-3D Pose Estimation

Robert M. Haralick and Hyonam Joo

Intelligent Systems Laboratory
Department of Electrical Engineering, FT-10
University of Washington
Seattle, WA 98195

ABSTRACT

In this paper we describe a robust technique for solving the 3D to 2D perspective projection pose estimation problem given corresponding point sets. The technique has considerable advantage over the least squares technique in that twenty or thirty percent of the corresponding point pair matches can be completely incorrect and the robust technique is able to determine the correct pose almost as accurately as the least squares technique if the least squares technique were to be given only the seventy to eighty percent correctly matched corresponding point pairs. Evidently, when the least squares technique is given a corresponding point pair data set with twenty or thirty percent of the corresponding pairs being incorrect matches, the technique becomes one of least virtue in the sense that the answer determined by least squares becomes virtually meaningless. Since computer vision procedures for determining corresponding point matches are notorious for being errorful, techniques for robust estimation of pose are important to have in the computer vision toolbox. Our conclusion about the robust technique are supported by hundreds of thousands of controlled experiments.

1. The Pose Estimation Problem

Let y_1, \dots, y_N be the observed 3D model points in Euclidean 3-space. Let R be a rotation matrix and t be a translation vector. Let $(u_{n1}, u_{n2}), n = 1, \dots, N$ be the corresponding 2D perspective projection of the 3D points. Then, the relationship between the 3D model points and the 2D perspective projection points is given by

$$u_{n1} = f \frac{r_1 y_n + t_1}{r_3 y_n + t_3}$$

$$u_{n2} = f \frac{r_2 y_n + t_2}{r_3 y_n + t_3}$$

$$t = (t_1, t_2, t_3)'$$

$$R = \begin{pmatrix} r_1 \\ r_2 \\ r_3 \end{pmatrix}$$

where f , the focal length, is the distance of the image plane in front of the origin which is the center of perspective.

In the 3D coordinate system of the camera, the perspective projections are given by

$$u_n = \begin{pmatrix} u_{n1} \\ u_{n2} \\ f \end{pmatrix} = f \begin{pmatrix} v_{n1} \\ v_{n2} \\ 1 \end{pmatrix} = f v_n$$

where $u_{n1} = f v_{n1}$ and $u_{n2} = f v_{n2}$.

The problem of pose estimation is to determine the unknown rotation matrix R and the translation vector t given the 3D model points and the corresponding 2D perspective projection points on the image plane. This problem is known as the exterior orientation problem in the photogrammetry literature. The dissertation by Szczepanski (1958) surveys nearly 80 different solutions beginning with one given by Schrieber of Karlsruhe in the year 1879. The first robust solution in the computer vision literature was Fischler and Bolles (1981). Wrobel and Klemm (1984) discuss the fact that there are configurations of points for which the solution is unstable.

2. The Iterative Least Squares Solution

This section describes iterative procedures for determining a least squares solution for R and t . In the following subsections, we use the superscript or subscript k to denote the values in the k^{th} iteration step. Let

$$x_n = \begin{pmatrix} x_{n1} \\ x_{n2} \\ x_{n3} \end{pmatrix} = R \begin{pmatrix} y_{n1} \\ y_{n2} \\ y_{n3} \end{pmatrix} + t$$

be the rotated and translated point of y_n . Let d_n be the estimated depth of each point x_n relative to the camera coordinate system.

2.1 Method 1

One iterative procedure for determining a least squares solution for R and t is

- (1) Choose initial reasonable values for the depth d_n^0 of each point. The initial values could, for example, be the same constant for each point, the constant representing an initial guess of how far the object is from the perspective center.

(2) Iterate. Suppose the depth values $d_n^k, n = 1, \dots, N$ are given. Define the depth values for the $(k+1)^{th}$ iteration by:

(2.1) Find the rotation matrix R_k and the translation vector t_k which minimizes

$$\epsilon_k^2 = \sum_{n=1}^N w_n \|R_k y_n + t_k - d_n^k v_n\|^2$$

where the $\{w_n \mid n = 1, \dots, N\}$ are non-negative weights reflecting the goodness of the observations. R_k and t_k constitute the solution to the 3D-3D pose estimation problem (Arun, 1987; Haralick et al., 1987).

(2.2) Define

$$d_n^{k+1} = \left(\frac{D_y}{D_x} \right) x_n^{k+1}$$

where

$$\begin{aligned} x_n^k &= R_k y_n + t_k \\ \bar{x} &= \frac{1}{N} \sum_{n=1}^N x_n, \quad \bar{y} = \frac{1}{N} \sum_{n=1}^N y_n \end{aligned}$$

and

$$\begin{aligned} D_y &= \sum_{n=1}^N \|y_n - \bar{y}\|^2 \\ D_x &= \sum_{n=1}^N \|x_n - \bar{x}\|^2 \end{aligned}$$

A typical convergence characteristic of the computed depth values is shown in Figure 4. This experiment is performed in a noise free environment with $N = 10$. The depth values of the first five points are plotted against the iteration number. The correct depth values are 33.27, 34.98, 38.81, 40.39, and 42.68.

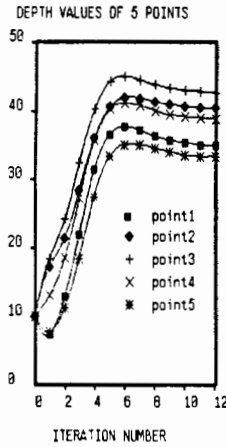


Figure 1 illustrates the convergence characteristics of Method 1. Convergence is achieved in about ten iterations.

2.2 Method 2

Replace the step (2.2) of Method 1 with (2.4).

(2.4) Define d_n^{k+1} by

$$d_n^{k+1} = \frac{(R_k y_n + t_k)' v_n}{v_n' v_n}$$

It can be shown that with this technique the residual squared error $\epsilon_{k+1}^2 \leq \epsilon_k^2$.

$$\begin{aligned} \epsilon_{k+1}^2 &= \sum_{n=1}^N w_n \|R_{k+1} y_n + t_{k+1} - d_n^{k+1} v_n\|^2 \\ &\leq \sum_{n=1}^N w_n \|R_k y_n + t_k - d_n^{k+1} v_n\|^2 \\ &= \sum_{n=1}^N w_n \|(x_n^k - d_n^k v_n) + (d_n^k v_n - d_n^{k+1} v_n)\|^2 \\ &= \sum_{n=1}^N w_n [\|(x_n^k - d_n^k v_n)\|^2 + 2(x_n^k - d_n^k v_n)'(d_n^k - d_n^{k+1})v_n \\ &\quad + (d_n^k - d_n^{k+1})^2 \|v_n\|^2] \\ &= \epsilon_k^2 + \sum_{n=1}^N w_n (d_n^k - d_n^{k+1}) [2(x_n^k - d_n^k v_n)' v_n \\ &\quad + (d_n^k - d_n^{k+1}) \|v_n\|^2] \\ &= \epsilon_k^2 + \sum_{n=1}^N w_n (d_n^k - d_n^{k+1}) [2x_n^{k'} v_n - 2d_n^k \|v_n\|^2 \\ &\quad + (d_n^k - d_n^{k+1}) \|v_n\|^2] \\ &= \epsilon_k^2 + \sum_{n=1}^N w_n (d_n^k - d_n^{k+1}) [2x_n^{k'} v_n - (d_n^k - d_n^{k+1}) \|v_n\|^2] \\ &= \epsilon_k^2 + \sum_{n=1}^N w_n \|v_n\|^2 \left[(d_n^{k+1})^2 - 2 \frac{x_n^{k'} v_n}{\|v_n\|^2} d_n^{k+1} \right. \\ &\quad \left. + 2 \frac{x_n^{k'} v_n}{\|v_n\|^2} d_n^k - (d_n^k)^2 \right] \\ &= \epsilon_k^2 + \sum_{n=1}^N w_n \|v_n\|^2 \left[\left(d_n^{k+1} - \frac{x_n^{k'} v_n}{\|v_n\|^2} \right)^2 - \left(d_n^k - \frac{x_n^{k'} v_n}{\|v_n\|^2} \right)^2 \right] \end{aligned}$$

Consider the terms in the bracket as a function of d_n^{k+1} . The function reaches a minimum when

$$d_n^{k+1} = \frac{x_n^{k'} v_n}{\|v_n\|^2}$$

The resulting value of the terms in the bracket at the minimum is

$$- \left(d_n^k - \frac{x_n^{k'} v_n}{\|v_n\|^2} \right)^2$$

This value cannot be positive. Since $w_n \|v_n\|^2 > 0$, when

$$d_n^{k+1} = \frac{x_n^{k'} v_n}{\|v_n\|^2}$$

each term in the summation is not positive and from this we can infer

$$\epsilon_{k+1}^2 \leq \epsilon_k^2$$

A typical convergence characteristic of the computed depth values is shown in Figure 5. This experiment is performed in a noise free environment with $N = 10$. The depth values of the first five points are plotted against the iteration number. Notice how the convergence is monotonic. The correct depth values are 33.27, 34.98, 38.81, 40.39, and 42.68.

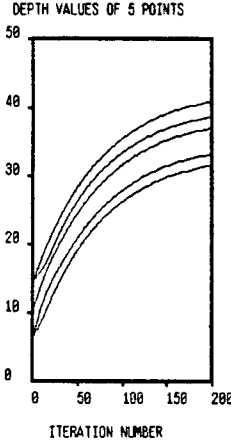


Figure 2 illustrates the convergence characteristics of Method 2. Convergence has been observed to be monotonic and is achieved in a few hundred iterations.

2.3 Least Squares Adjustment by Linearization

Let ϕ, θ , and ψ be the three angles that define the rotation matrix R such that

$$R = R_z(\phi)R_y(\theta)R_x(\psi)$$

$$= \begin{pmatrix} \cos \theta \cos \psi & \cos \theta \sin \psi & -\sin \theta \\ -\cos \phi \sin \psi + \sin \phi \sin \theta \cos \psi & \cos \phi \cos \psi + \sin \phi \sin \theta \sin \psi & \sin \phi \cos \theta \\ \sin \phi \sin \psi + \cos \phi \sin \theta \cos \psi & -\sin \phi \cos \psi + \cos \phi \sin \theta \sin \psi & \cos \phi \cos \theta \end{pmatrix}$$

As there always exists random errors in the measurement of the image coordinates, let

$$u_{ni} = u_{ni}^0 + \nu_{ni}, \quad i = 1, 2, \quad n = 1, \dots, N$$

where (u_{n1}^0, u_{n2}^0) are the measured image points and (ν_{n1}, ν_{n2}) are the corrections needed to account for the random error in the measured coordinates. Similarly, let

$$\begin{aligned} \phi &= \phi^0 + \Delta\phi \\ \theta &= \theta^0 + \Delta\theta \\ \psi &= \psi^0 + \Delta\psi \\ t_i &= t_i^0 + \Delta t_i, \quad i = 1, 2, 3 \end{aligned}$$

where $\phi^0, \theta^0, \psi^0, t_1^0, t_2^0$ and t_3^0 are some approximations, and $\Delta\phi, \Delta\theta, \Delta\psi, \Delta t_1, \Delta t_2$ and Δt_3 are their corresponding corrections. We assume that the corrections Δ 's are small and the collinearity equations are linear over the small intervals between the true values of these parameters and their corresponding approximation.

Let

$$F_{n1} = u_{n1} - f \frac{r_1 y_n + t_1}{r_3 y_n + t_3}$$

$$F_{n2} = u_{n2} - f \frac{r_2 y_n + t_2}{r_3 y_n + t_3}$$

These equations can be linearized by Newton's first order approximation as follows:

$$\begin{aligned} F_{n1} &\simeq F_{n1}^0 + \nu_{n1} + b_{n11}\Delta\phi + b_{n12}\Delta\theta + b_{n13}\Delta\psi \\ &\quad + b_{n14}\Delta t_1 + b_{n15}\Delta t_2 + b_{n16}\Delta t_3 \\ F_{n2} &\simeq F_{n2}^0 + \nu_{n2} + b_{n21}\Delta\phi + b_{n22}\Delta\theta + b_{n23}\Delta\psi \\ &\quad + b_{n24}\Delta t_1 + b_{n25}\Delta t_2 + b_{n26}\Delta t_3 \end{aligned}$$

where

$$\begin{aligned} b_{n11} &= \left(\frac{\partial F_{n1}}{\partial \phi} \right)^0, & b_{n12} &= \left(\frac{\partial F_{n1}}{\partial \theta} \right)^0 \\ b_{n13} &= \left(\frac{\partial F_{n1}}{\partial \psi} \right)^0, & b_{n14} &= \left(\frac{\partial F_{n1}}{\partial t_1} \right)^0 \\ b_{n15} &= \left(\frac{\partial F_{n1}}{\partial t_2} \right)^0, & b_{n16} &= \left(\frac{\partial F_{n1}}{\partial t_3} \right)^0 \end{aligned}$$

for $i = 1, 2$, where the superscript 0 implies that the function values are computed with the approximations $(\phi^0, \theta^0, \psi^0, t_1^0, t_2^0, t_3^0)$. In matrix notation, the linearized equation can be expressed as

$$\begin{pmatrix} b_{111} & b_{112} & b_{113} & b_{114} & b_{115} & b_{116} \\ b_{121} & b_{122} & b_{123} & b_{124} & b_{125} & b_{126} \\ \vdots & \vdots & \vdots & \vdots & \vdots & \vdots \\ b_{N11} & b_{N12} & b_{N13} & b_{N14} & b_{N15} & b_{N16} \\ b_{N21} & b_{N22} & b_{N23} & b_{N24} & b_{N25} & b_{N26} \end{pmatrix} \begin{pmatrix} \Delta\phi \\ \Delta\theta \\ \Delta\psi \\ \Delta t_1 \\ \Delta t_2 \\ \Delta t_3 \end{pmatrix} =$$

$$\begin{pmatrix} -F_{11}^0 \\ -F_{12}^0 \\ \vdots \\ -F_{N1}^0 \\ -F_{N2}^0 \end{pmatrix} - \begin{pmatrix} \nu_{11} \\ \nu_{12} \\ \vdots \\ \nu_{N1} \\ \nu_{N2} \end{pmatrix}$$

or simply

$$B\Delta = F - \nu$$

This equation can be solved using the singular value decomposition method. The computed corrections $\Delta = (\Delta\phi, \Delta\theta, \Delta\psi, \Delta t_1, \Delta t_2, \Delta t_3)'$ from one iteration are used to update the parameters $\Lambda = (\phi^0, \theta^0, \psi^0, t_1^0, t_2^0, t_3^0)'$ and then these updated parameters are used as approximations in the next iteration. The whole iteration process is repeated until the corrections becomes negligibly small.

2.4 Robust M-Estimation

This section describes some robust techniques used in nonlinear regression problems. In particular, it can be used to solve robustly the equation $B\Delta = F - \nu$ which results from the linearization of the original pose estimation problem. Any estimate T_k defined by a minimization problem of the form.

$$\min_{T_k} \sum_{i=1}^n \rho(x_i - T_k)$$

or by an implicit equation

$$\sum_{i=0}^n \psi(x_i - T_k) = 0$$

where ρ is an arbitrary non-negative function (called object function),

$$\psi(x - T_k) = \frac{\partial}{\partial T_k} \rho(x - T_k)$$

is called an M-estimate. This last equation can be written equivalently as

$$\sum_{i=0}^n w_i(x_i - T_k) = 0$$

where

$$w_i = \frac{\psi(x_i - T_k)}{x_i - T_k}, \quad i = 1, \dots, n$$

this gives a formal representation of T_k as a weighted mean

$$T_k = \frac{\sum_{i=1}^n w_i x_i}{\sum_{i=1}^n w_i}$$

with weights depending on the sample (Huber, 1981). It is known that M-estimators minimize objective functions more general than the familiar sum of squared residuals associated with the sample mean. Among many forms of functions ρ and ψ proposed in the literature, Huber's and Tukey's form is investigated in the experiments described in this paper. Huber derived the following robust ρ and ψ .

$$\rho(x) = \begin{cases} 0.5x^2, & \text{if } |x| \leq a; \\ a|x| - 0.5a^2, & \text{otherwise.} \end{cases}$$

$$\psi(x) = \begin{cases} -a, & \text{if } x < -a; \\ x, & \text{if } |x| \leq a; \\ a, & \text{if } x > a. \end{cases}$$

Tukey's ψ function can be expressed as

$$\psi(x) = \begin{cases} x \left(1 - \left(\frac{x}{a}\right)^2\right)^2, & \text{if } |x| \leq a; \\ 0, & \text{if } |x| > a. \end{cases}$$

where a is a tuning constant, 1.5 for Huber's and 6 for Tukey's.

The nonlinear regression problem can be formulated as follows. Let $f_i : E^m \rightarrow E$, $i = 1, \dots, n$ be functions that map m -dimensional space into a real line. Let $\theta = (\theta_1, \theta_2, \dots, \theta_m)' \in E^m$ be the m -dimensional unknown vector to be estimated. The solution to the set of n equations

$$f_i(\theta) = y_i, \quad i = 1, \dots, n$$

which minimizes

$$\sum_{i=1}^n \rho \left(\frac{y_i - f_i(\theta)}{S} \right)$$

can be found in several different ways. To create a scale invariant version of the M-estimator, the robust estimate of scale such as the following is introduced.

$$S = \frac{\text{median}_i |y_i - f_i(\theta)|}{0.6745}$$

where 0.6745 is one half of the interquartile range of the Gaussian normal distribution $N(0,1)$. Here we take the median of the nonzero deviations only because, with large n , too many residuals can equal zero (Hogg, 1979).

In robust estimation, the estimates are obtained only after an iterative process because the estimates do not have closed forms. Two such iterative methods are presented here that can solve the minimization problem stated above (Huber, 1981).

2.4.1 Modified Residual Method

In this method, the residuals are modified by a proper ψ function before the least squares problem is solved. The iterative procedure to determine θ is

- (1) Choose an initial approximation θ^0 .
- (2) Iterate. Given the estimation θ^k in step k , compute the solution in the $(k+1)$ th step as follows.

- (2.1) Compute the modified residuals r_i^* for $i = 1, \dots, n$.

$$r_i^* = \psi \left(\frac{r_i}{S^k} \right) S^k$$

where

$$r_i = y_i - f_i(\theta^k)$$

$$S^k = \frac{\text{median}_{r_i \neq 0} |r_i|}{0.6745}$$

- (2.2) Solve the least squares problem $X\delta = r^*$. where $X = [x_{ij}]$ is the gradient matrix.

$$x_{ij} = \frac{\partial}{\partial \theta_j} f_i(\theta^k)$$

The solution for this equation can be found using the standard least squares method. If the singular value decomposition of the matrix X is $X = U_1 \Sigma_1 V'$, then the solution is $\hat{\delta} = V \Sigma_1^{-1} U_1' r^*$.

- (2.3) Set $\theta^{k+1} = \theta^k + \hat{\delta}$.

2.4.2 Modified Weights Method

Taking the derivative of the objective function ρ with respect to θ and set it to zero, we get

$$\sum_i \psi \left(\frac{y_i - f_i(\theta)}{S} \right) \frac{\partial f_i(\theta)}{\partial \theta_j} = 0$$

In the standard weighted form

$$\sum_i w_i r_i \frac{\partial f_i(\theta)}{\partial \theta_j} = 0$$

where

$$w_i = \frac{\psi \left(\frac{r_i}{S} \right)}{\left(\frac{r_i}{S} \right)}$$

Therefore, the iterative procedure to determine θ is

- (1) Choose an initial approximation θ^0 .

(2) Iterate. Given θ^k at k th step, compute θ^{k+1} as follows.

(2.1) Solve

$$PX\delta = Pr$$

where

$$P = \begin{pmatrix} \sqrt{w_1} & & \\ & \ddots & \\ & & \sqrt{w_N} \end{pmatrix}$$

(2.2) If $\hat{\delta}$ is the solution in step (2.1), then set

$$\theta^{k+1} = \theta^k + \hat{\delta}$$

3. Experimental Results

To measure the performance of the pose estimation algorithms, several hundred thousand controlled experiments were performed. This section describes how the controlled experiments are constructed and shows the results from those experiments. The results are presented as graphs where the sum of errors of the three rotation angles, ϕ, θ, ψ , is plotted against various control parameters such as the signal to noise ratio (SNR), the number of matched points, or the number of outliers, which will be defined later.

3.1 Data Set Generation

A set of 3D model points, $y_i = (y_{i1}, y_{i2}, y_{i3})', i = 1, \dots, N$, are generated within a box defined by

$$y_{i1}, y_{i2}, y_{i3} \in [0, 10]$$

That is, each of the three coordinates are independent random variables each of them uniformly distributed between 0 and 10. Next, three rotation angles are selected from an interval $[20, 70]$ and the translation vector $t = (t_1, t_2, t_3)$ is also generated such that t_1 and t_2 are uniformly distributed within an interval $[5, 15]$ and t_3 is within $[20, 50]$. Having these transformation parameters, the 3D model points are rotated and translated in the 3D space forming a set of 3D points $x_i, i = 1, \dots, N$. At this stage, independent identically distributed Gaussian noise $N(0, \sigma)$ is added to all three coordinates of the transformed points x_i . To test the robustness of the algorithms, some fraction of the 3D points, x_i , are replaced with randomly generated 3D points, $z_i = (z_{i1}, z_{i2}, z_{i3})', i = 1, \dots, M$. M is the number of the replaced 3D points and

$$z_{i1} = t_1 + \nu_{i1}$$

$$z_{i2} = t_2 + \nu_{i2}$$

$$z_{i3} = x_{i3}$$

where $\nu_{i1}, \nu_{i2}, i = 1, \dots, M$ are independent random variables uniformly distributed within an interval $[-5, 5]$. These random points, z_i , are called outliers in our experiments. To get the matching set of 2D points, $x_i, i = 1, \dots, N$ are perspective projected onto the image plane. Given the 3D model points and the corresponding 2D points on the image plane, each algorithm is applied to find the three rotation

angles and the translation vector.

One can notice from the above description that there are three parameters we can control in each experiment. They are the number of 3D model points N , the standard deviation σ of the Gaussian noise, and the number of outliers M . In the experimental result, we use SNR and the percent of outliers PO, in place of σ and M respectively, where

$$\text{SNR} = 20 \log \frac{10}{\sigma} \text{db}$$

$$\text{PO} = \frac{M}{N} \times 100\%$$

3.2 Results

For each parameter setting, (N , SNR, PO), 1000 experiments are performed to get a reasonable estimate of the performance of the algorithms. For each algorithm, we performed three different sets of experiments (E1, E2, and E3), as follows.

- E1: Set $N = 20$. Estimate the sum of the three rotation angle errors against SNR (20db to 80db in 10db step) for different PO (0% to 20% in 5% step).
- E2: Set SNR = 40db. Estimate the sum of the three rotation angle errors against PO (0% to 20% in 5% step) for different N (10 to 50 by steps of 10).
- E3: Set PO = 10%. Estimate the sum of the three rotation angle errors against SNR (20db to 80db in 10db step) for different N (10 to 50 by steps of 10).

Figure 6 shows the results of E1, E2, and E3 performed for the initial approximation algorithm using iterative least squares solution (A1), Method 2 of section 2.2. Initial estimates for the approximating depth are set to 10 in all experiments. For the linearized algorithms, the initial estimate of the three rotation angles are selected randomly within 15 degrees of the true angles. The initial approximate of the translation vector is selected randomly within ± 10 of the true translation vector. Figures 7 and 8 show the result of the least squares adjustment by linearization algorithm (A2), algorithm in section 2.3, and the robust M-estimate algorithm (A3), modified weights algorithm in section 2.4.2, respectively. Figure 9 compares the three algorithms A1, A2, and A3 in the experiment set E1. Figures 10 and 11 compare the three algorithms in the experiment set E2 and E3 respectively. One more experiment compares the algorithms A2 and A3. With $N = 20$ and PO = 10%, algorithms A2 and A3 are applied for SNR from 20db to 40db in a step of 10db, and the algorithm A2 is applied for $N = 18$, PO = 0% and SNR from 20db to 40db in a step of 10db. This compares the efficiency of the robust technique against the non-robust technique in the case where the non-robust technique uses only the non-outlier points given to the robust technique. Figure 12 shows the result of this experiment.

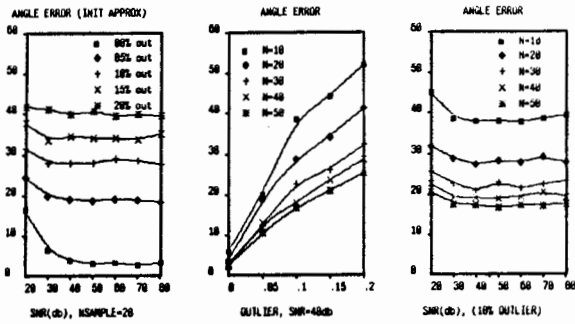


Figure 3 illustrates the performance characteristics for the initial approximation solution (Method 2).

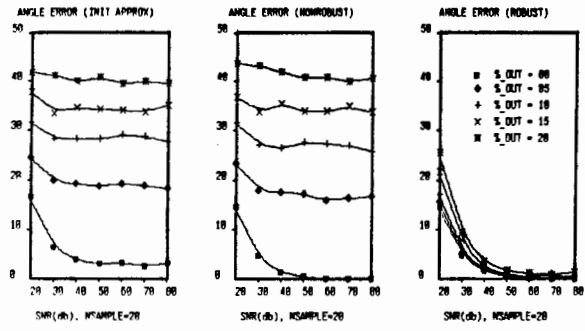


Figure 6 illustrates the performance characteristics of angle error as a function of signal to noise ratio for the initial approximation method, the non-robust linearized least squares adjustment, and the robust M-estimate.

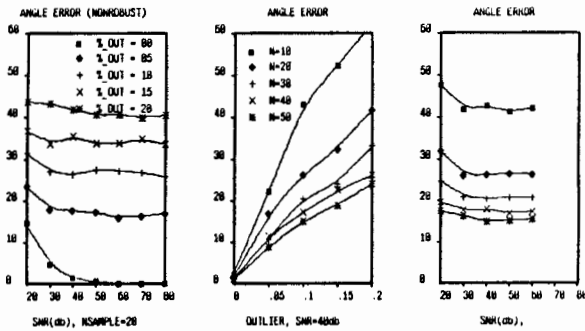


Figure 4 illustrates the performance characteristics of the least squares adjust by linearization.

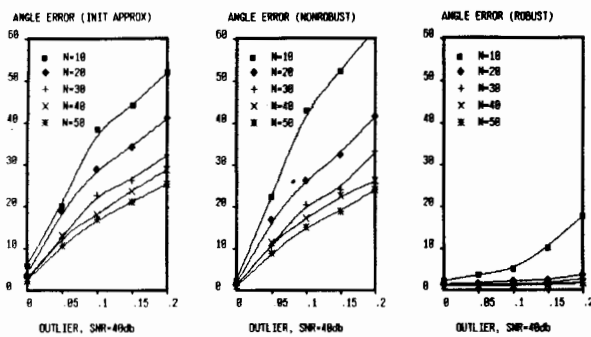


Figure 7 illustrates the performance characteristics of angle error versus fraction of outliers for the initial approximation method, the linearized least squares adjustment, and the robust M-estimate.

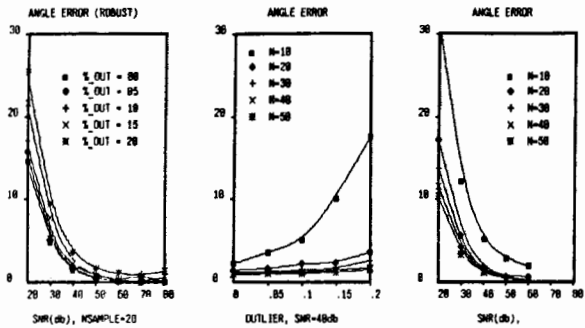


Figure 5 illustrates the performance characteristics of the robust M-estimate algorithm.

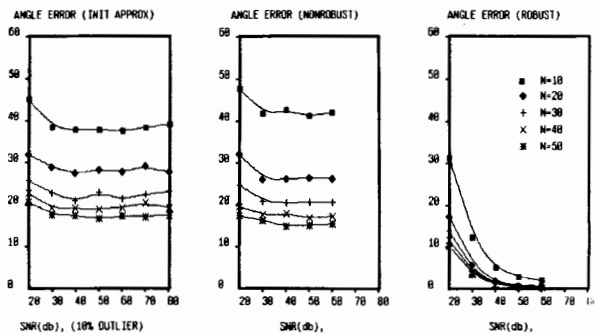


Figure 8 illustrates the performance characteristics of angle error versus fraction of outliers for the initial approximation method, the linearized least squares adjustment, and the robust M-estimate.

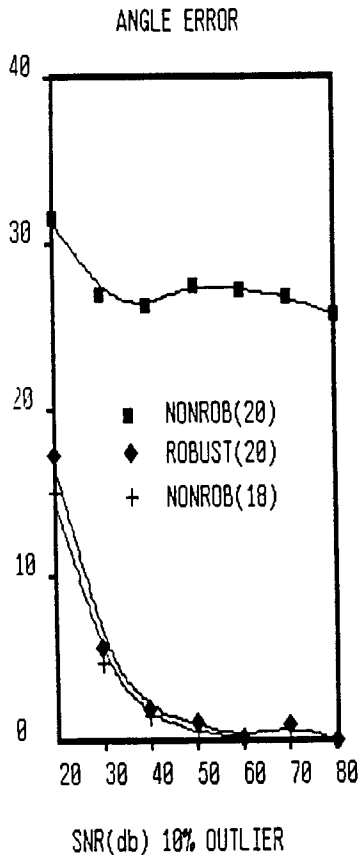


Figure 9 illustrates the efficiency of the robust technique operating on a data set of 20 points, 18 points having Gaussian noise and 2 outliers, against the non-robust technique operating on a data set having 18 points having Gaussian noise.

4. References

1. Arun, K.S., T.S. Huang, and S.D. Blostein, "Least-Squares Fitting of Two 3-D Point Sets," *IEEE Transactions on Pattern Analysis and Machine Intelligence*, Vol. PAMI-9, No.4, 1987, pp. 698-700.
2. Fischler, Martin A. and Robert C. Bolles, "Random Sample Consensus: A Paradigm for Model Fitting with Applications to Image Analysis and Automated Cartography," *Communications of the ACM*, Vol. 24, No. 6, 1981, pp. 381-395.
3. Haralick, R.M., C.N.Lee, X. Zhuang, V.G. Vaidya, and M.B. Kim, "Pose Estimation from Corresponding Point Data," *Workshop on Computer Vision*, Miami Beach, FL, , November 30-December 2, 1987, pp. 258-263.
4. Hogg, Robert V., *An Introduction to Robust Estimation, Robustness in Statistics*, R.L. Launer & G.N. Wilkinson (Eds.),
5. Huber, Peter J., *Robust Statistics*, John Wiley & Sons, 1981.
6. Szczepanski, W., "Die Lösungsvorschlaege für den räumlichen Rückwärtseinschnitt," *Deutsche Geodätische Kommission, Reihe C: Dissertationen—Heft Nr. 29*, 1958, 1-144.
7. Wrobel, B., and D. Klemm, "Über der Berechnung allgemeiner räumlicher Drehungen," *International Archives of Photogrammetry and Remote Sensing*, Vol. 25, Part A3b, pp. 1153-1163.